

Supporting Information

Hydroxyl-assisted ionic bifunctional hyper-crosslinked polymer as an efficient and recyclable heterogeneous catalyst for CO₂ cycloaddition

Jingjing Liu,^{‡a} Shulei Xiang,^{‡a} Dexuan Xiang,^{a,c*} Jingao Wu,^{a,c} Hongliang Xu,^b Gui Chen,^a Zaixing Zhang^{a,c}, Feipeng Yuan and Yuejun Ouyang^{a,c}

^a College of Chemistry and Materials, Huaihua University, Huaihua 418000, P. R. China

^b Institute of Functional Material Chemistry, Department of Chemistry, Northeast Normal University, Changchun, 130024, People's Republic of China.

^c Key Laboratory of Preparation and Application of Environmentally Friendly Functional Materials, Huaihua University, Huaihua 418000, P. R. China

* Corresponding author

Tel.: +86-745-2851014.

‡Jingjing Liu and Shulei Xiang contributed equally to this work.

E-mail address: dexuanxiang@126.com (D.Xiang)

1. Experimental

1.1 Reagents

The macroporous chloromethylated polystyrene (CMPs), with a chlorine content of 17.3% (w/w), was obtained from Langfang Chemical Co. Ltd., China. Reagents such as 4-hydroxypyridine (AR, 97%), potassium carbonate (AR, 98%), iron chloride (FeCl_3 , AR, 99.9%), dimethoxymethane (FDA, AR, 98.0%), dimethylformamide (DMF, AR, 98.0%), and epoxides (AR) were acquired from Shanghai Aladdin Biochemical Technology Co., Ltd., China. Additionally, 1,2-dichloroethane (AR, 99.5%) was sourced from Chengdu Jinshan Chemical Co., Ltd., China. Unless otherwise specified, all other chemicals were purchased commercially and used directly without additional purification.

1.2 Characterizations

The XPS spectra were measured with a Thermo ESCALAB 250XI under the stimulation of Al Ka radiation. For Fourier transform infrared (FT-IR) spectra, they were obtained from 400 cm^{-1} to 4000 cm^{-1} by means of the FT-IR Bruker (EQUINOX 55) spectrometer. The Micromeritics ASAP 2460 surface area and porosity analyzer was utilized to record the specific surface area (S_{BET}) and pore size distributions via the N_2 adsorption-desorption isotherms. The TGA was executed on a DSC Q2000 within an N_2 gas atmosphere, with the temperature ranging from ambient to 800 °C. The morphology of the resins was examined by SEM (Zeiss, Sigma

HD) and TEM (FEI Tecnai G20). The XRD spectra were collected using a Rigaku Ultima IV X-ray diffractometer with Cu K α radiation (40 kV and 40 mA). The elemental analyzer (UNICUBE) was employed to test the C/N/H/O contents, while the Cl contents were determined through the Volhard method. The products underwent purification by column chromatography. The ^1H NMR spectra were detected at 400 MHz, with TMS serving as the internal standard, on a Quantum-I Plus 400 MHz spectrometer.

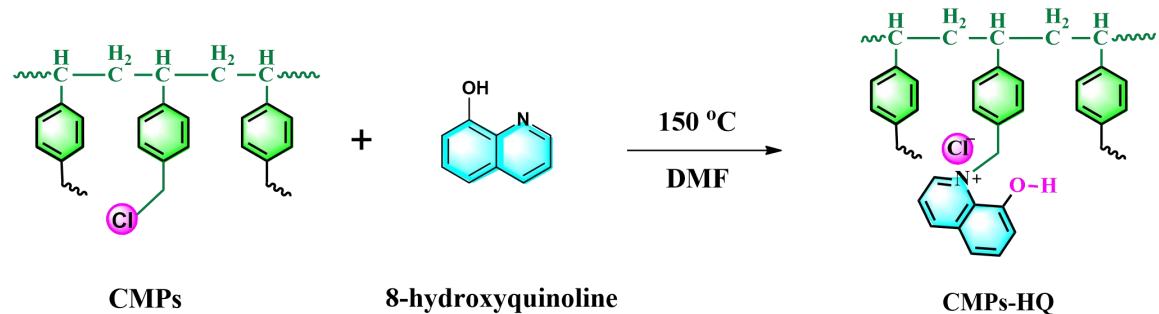
1.3 Computational methods

The first-principles calculations were performed using the Vienna ab initio simulation package (VASP)^[1, 2] based on density-functional theory (DFT) with the projector augmented wave (PAW) method^[3]. The generalized gradient approximation (GGA-PBE) functional of Perdew-Burke-Ernzerhoff (PBE)^[4, 5] was utilized to define the exchange-correlation interaction. Spin calculations were adopted. A cutoff energy of 450 eV was applied to the plane-wave basis. Structural relaxation was attained using the conjugate gradient (CG) method, iterated until the total energy error was below 10^{-5} eV, and the force on each atom was less than 0.02 eV/Å. The Brillouin zone was sampled using a single gamma k-point grid. To optimize the minimum-energy path (MEP), the climbing image nudged elastic band (CINEB) method¹ was employed to pinpoint the transition state, imposing a force convergence criterion on each atom of 0.03eV/ Å.

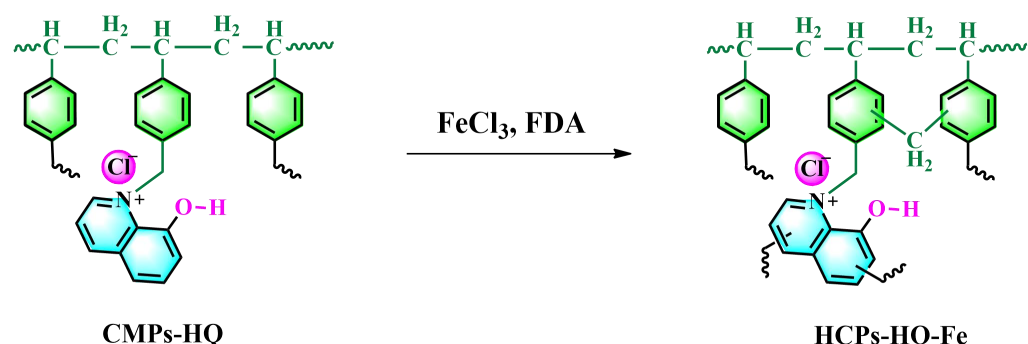
References:

- [1] KRESSE G, FURTHMÜLLER J. Efficient iterative schemes for ab initio total-energy calculations using a plane-wave basis set [J]. *Physical Review B*, 1996, 54(16): 11169-11186.
- [2] KRESSE G, HAFNER J. Ab initio molecular-dynamics simulation of the liquid-metal--amorphous-semiconductor transition in germanium [J]. *Physical Review B*, 1994, 49(20): 14251-14269.
- [3] BLÖCHL P E. Projector augmented-wave method [J]. *Physical Review B*, 1994, 50(24): 17953-17979.
- [4] PERDEW J P, BURKE K, ERNZERHOF M. Generalized gradient approximation made simple [J]. *Physical review letters*, 1996, 77(18): 3865.
- [5] PERDEW J P, BURKE K, ERNZERHOF M. Erratum: Generalized gradient approximation made simple (Physical Review Letters (1996) 77 (3865)) [J]. *Physical Review Letters*, 1997, 78(8): 1396.

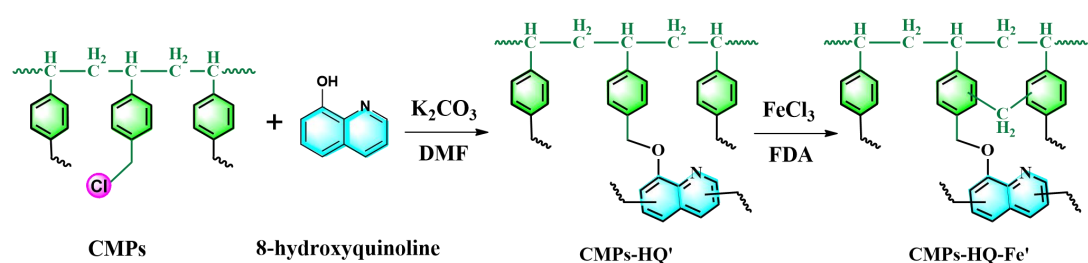
1.4 Scheme S1. Synthesis of CMPs-HQ



1.5 Scheme S2. Synthesis of HCPs-HQ-Fe



1.6 Scheme S3. Synthesis of HCPs-HQ-Fe'

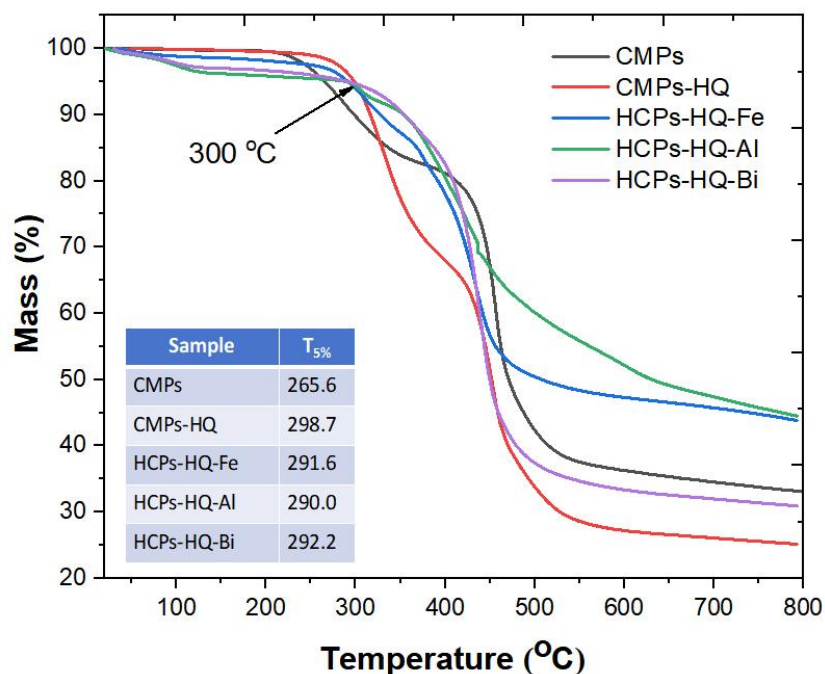


1.7 Scheme S4. Synthesis of HCPs-Q-Fe

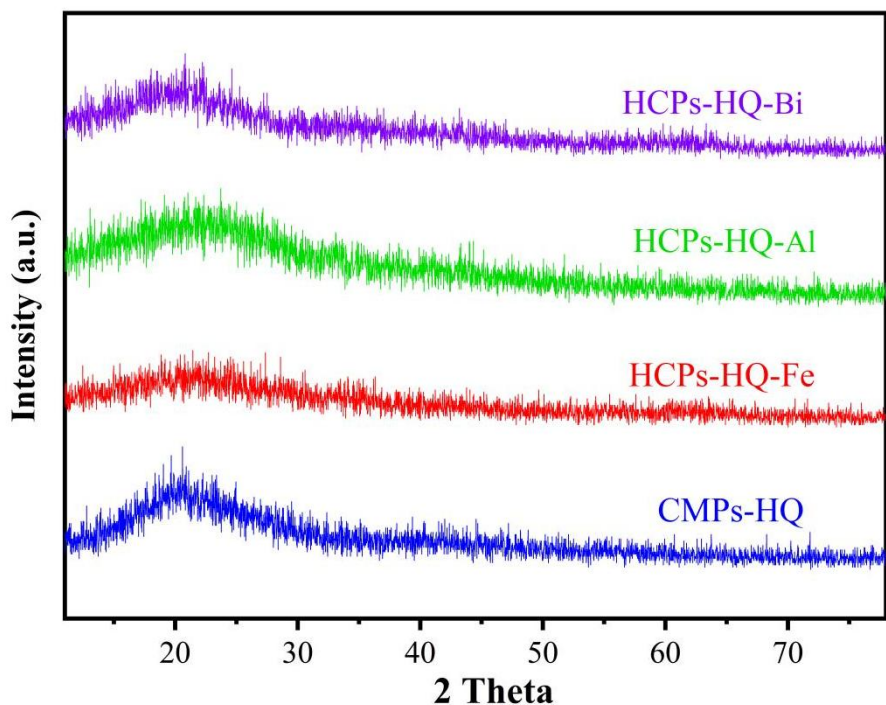


2. Catalyst characterizations

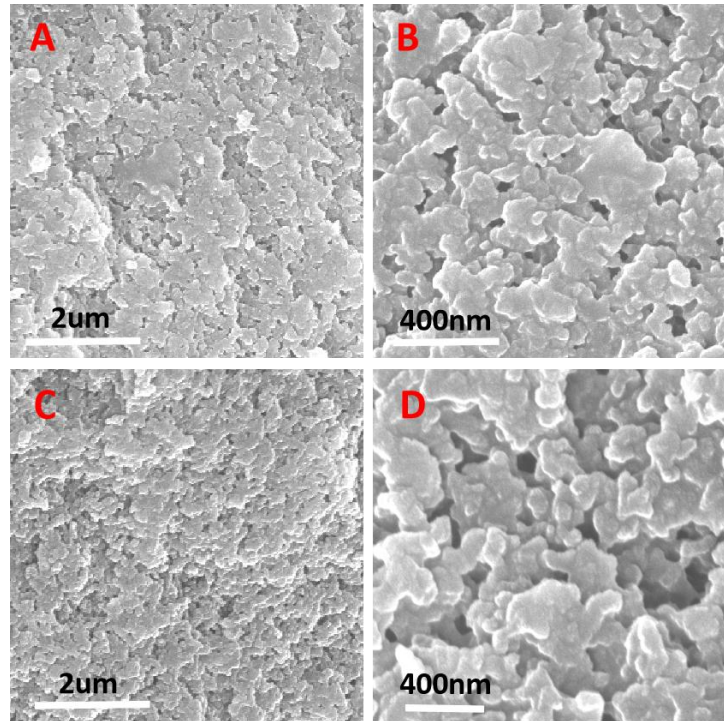
2.1 Fig. S1. TGA curves of samples



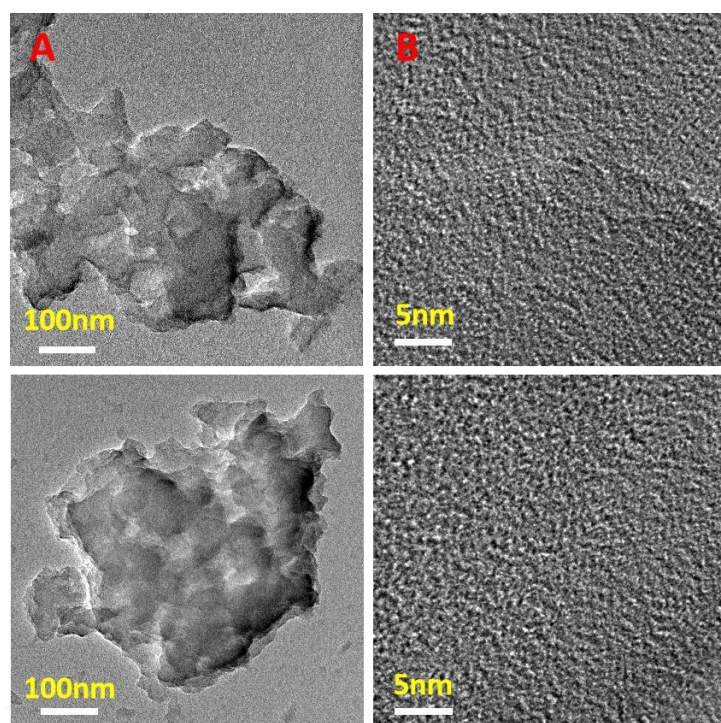
2.2 Fig. S2. XRD patterns of CMPs-HQ and HCPs-HQ



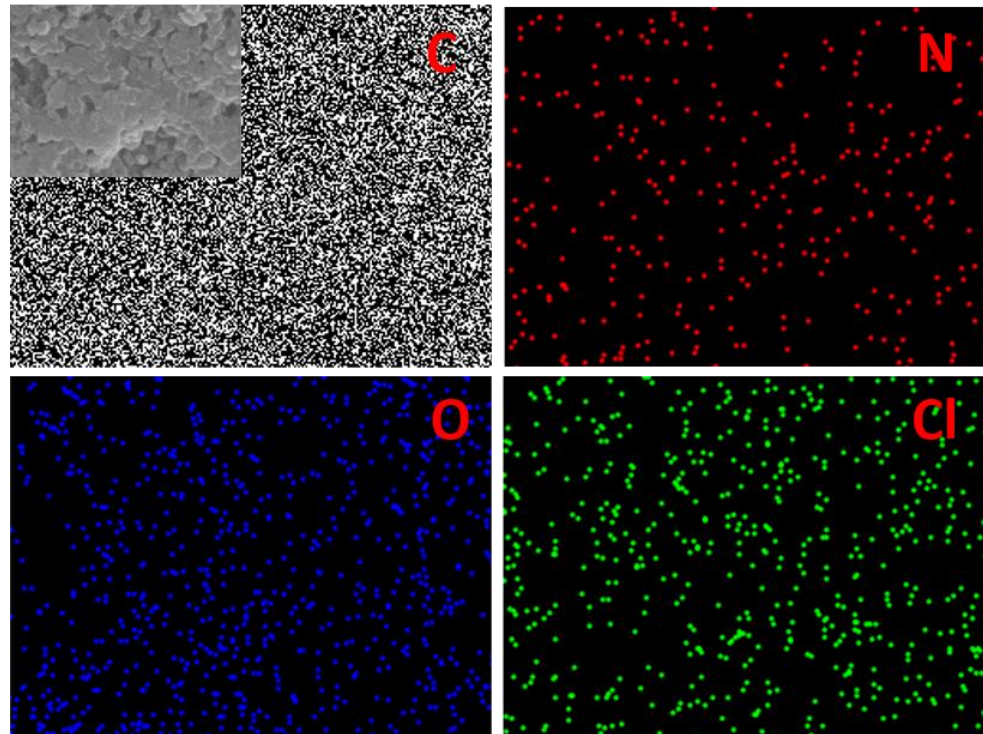
2.3 Fig. S3. SEM image of HCPs-HQ-Al (A and B) and HCPs-HQ-Bi (C and D)



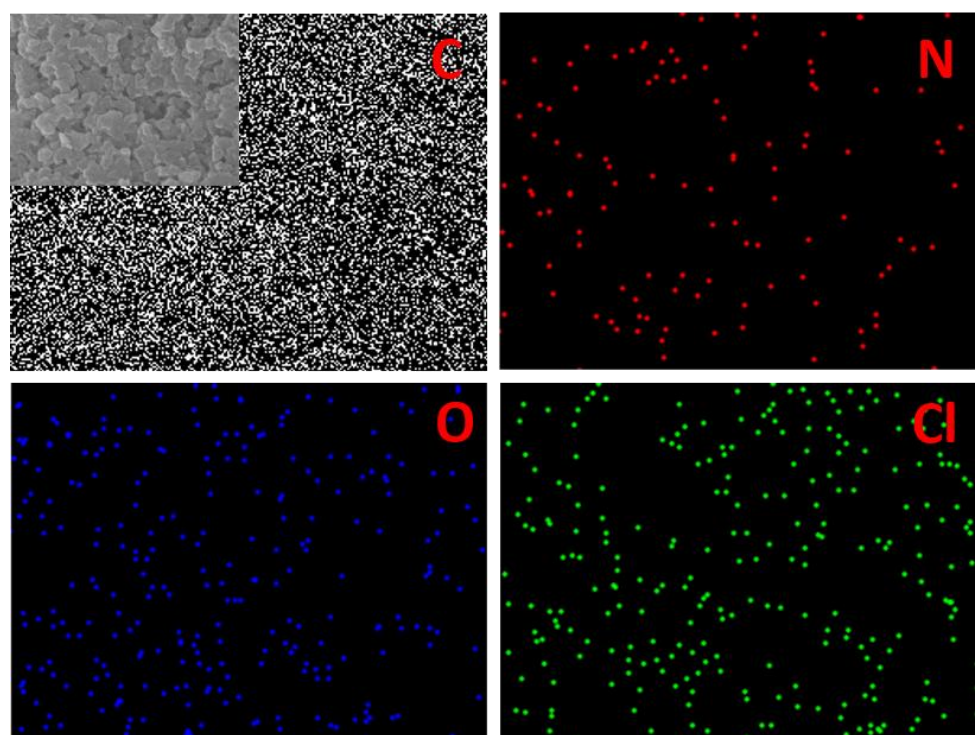
2.4 Fig. S4. TEM image of HCPs-HQ-Al (A and B) and HCPs-HQ-Bi (C and D)



2.5. Fig. S5. SEM-Mapping images of HCPs-HQ-Al : Carbon (grey), Nitrogen (blue), Oxygen (red), and Chlorine green).



2.6 Fig. S6. SEM-Mapping images of HCPs-HQ-Bi : Carbon (grey), Nitrogen (blue), Oxygen (red), and Chlorine green).



3. Application in the CO₂-epoxide cycloaddition reaction

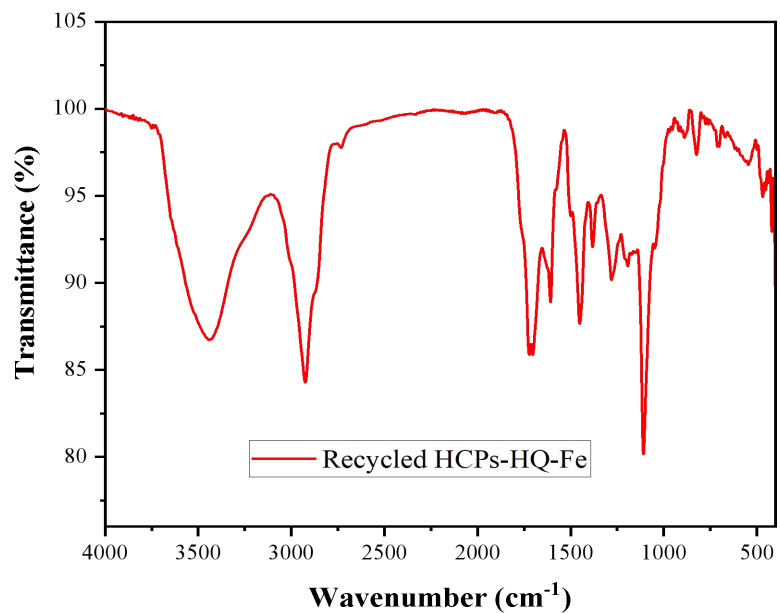
Table S1 Optimization of the cycloaddition condition ^a

Entry	Catalyst	Dosage	Pressure	Temp. °C	Time	Yield ^b		
						g	MPa	h
1	HCPs-HQ-Fe	0.1	1.0	80	10	56		
2	HCPs-HQ-Al	0.1	1.0	80	10	48		
3	HCPs-HQ-Bi	0.1	1.0	80	10	43		
4	HCPs-HQ-Fe	0.1	1.0	60	10	18		
5	HCPs-HQ-Fe	0.1	1.0	100	10	86		
6	HCPs-HQ-Fe	0.1	1.0	120	10	96		
7	HCPs-HQ-Fe	0.1	1.0	100	20	99		
8	HCPs-HQ-Fe	0.1	0.1	100	20	99		
9	HCPs-HQ-Fe	0.02	0.1	100	20	99		
10	HCPs-HQ-Fe	0.01	0.1	100	20	90		
11	HCPs-HQ-Al	0.02	0.1	100	20	93		
12	HCPs-HQ-Bi	0.02	0.1	100	20	88		
13	CMPs-HQ	0.02	0.1	100	20	26		
14	CMPs	0.02	0.1	100	20	0		
15	HCPs-Q-Fe	0.02	0.1	100	20	23		
16	HCPs-HQ-Fe'	0.02	0.1	100	20	4		

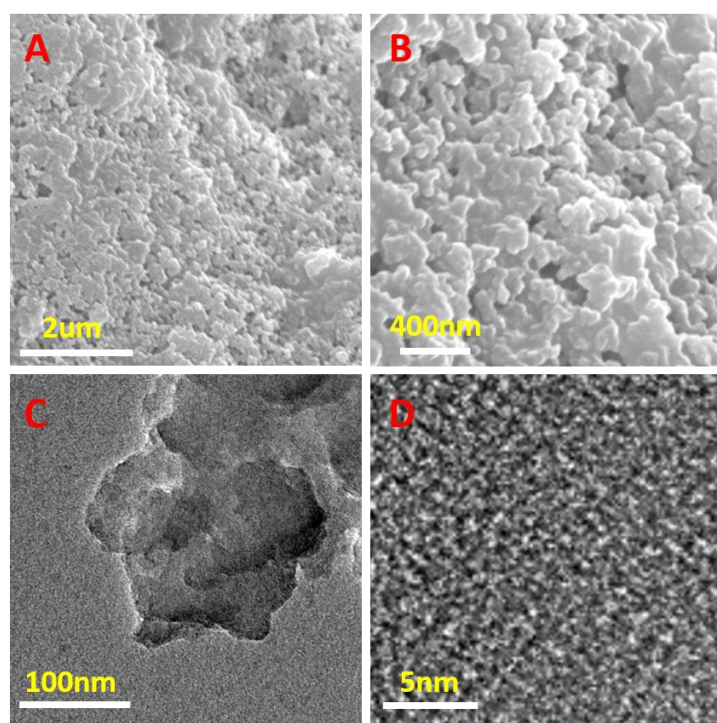
^aReaction conditions: epichlorohydrin (3.0 g). ^bThe yield is characterized by ¹H NMR.

4. Catalyst recycling

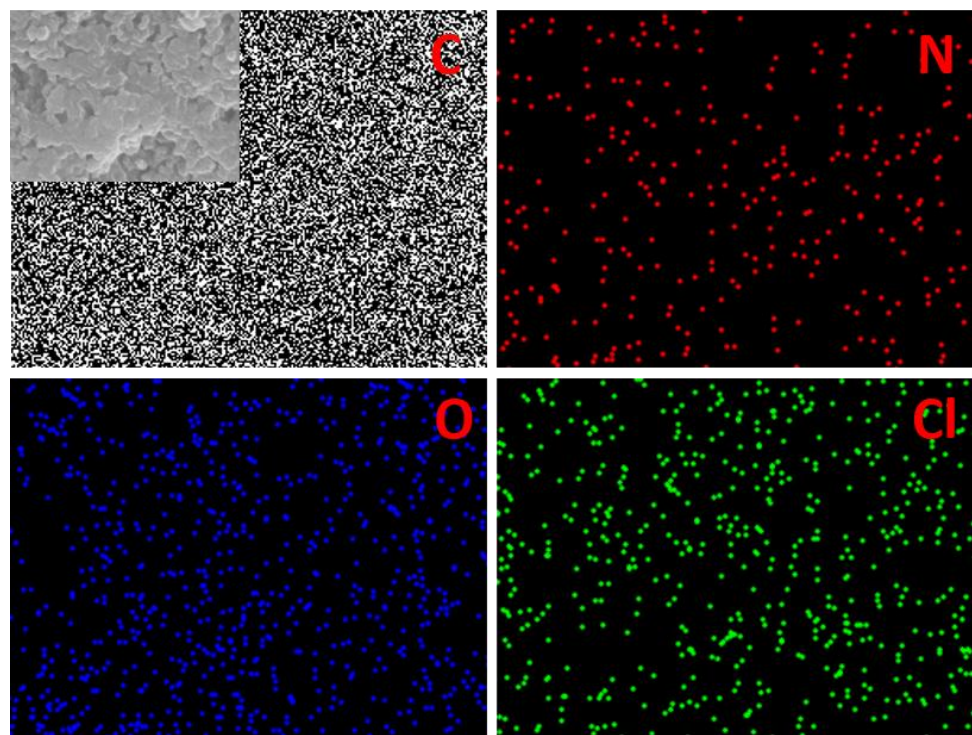
4.1 Fig. S7 FT-IR spectra of recycled HCPs-HQ-Fe.



4.2 Fig. S8 SEM images (A and B) and TEM images (A and B) of recycled HCPs-HQ-Fe.



4.3 Fig. S9. SEM-Mapping images of recycled HCPs-HQ-Fe.



5. FT-IR spectra of recycled HCPs-HQ-Fe' and HCPs-Q-Fe.

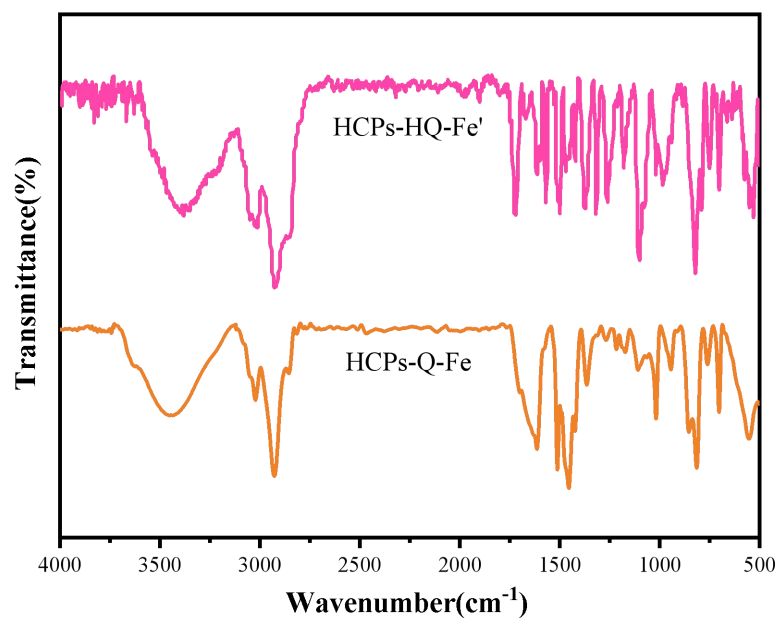


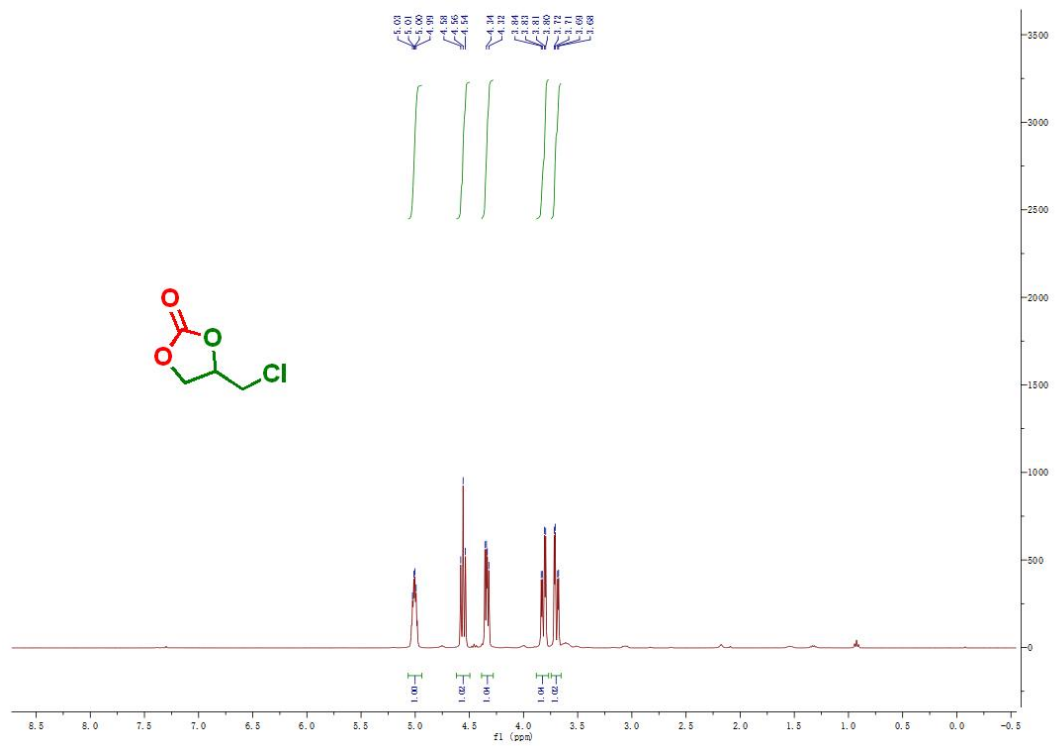
Fig. S10 FT-IR spectra of recycled HCPs-HQ-Fe' and HCPs-Q-Fe.

6. Table S2. Elemental analysis of HCPs-HQ-Fe and recycled HCPs-HQ-Fe

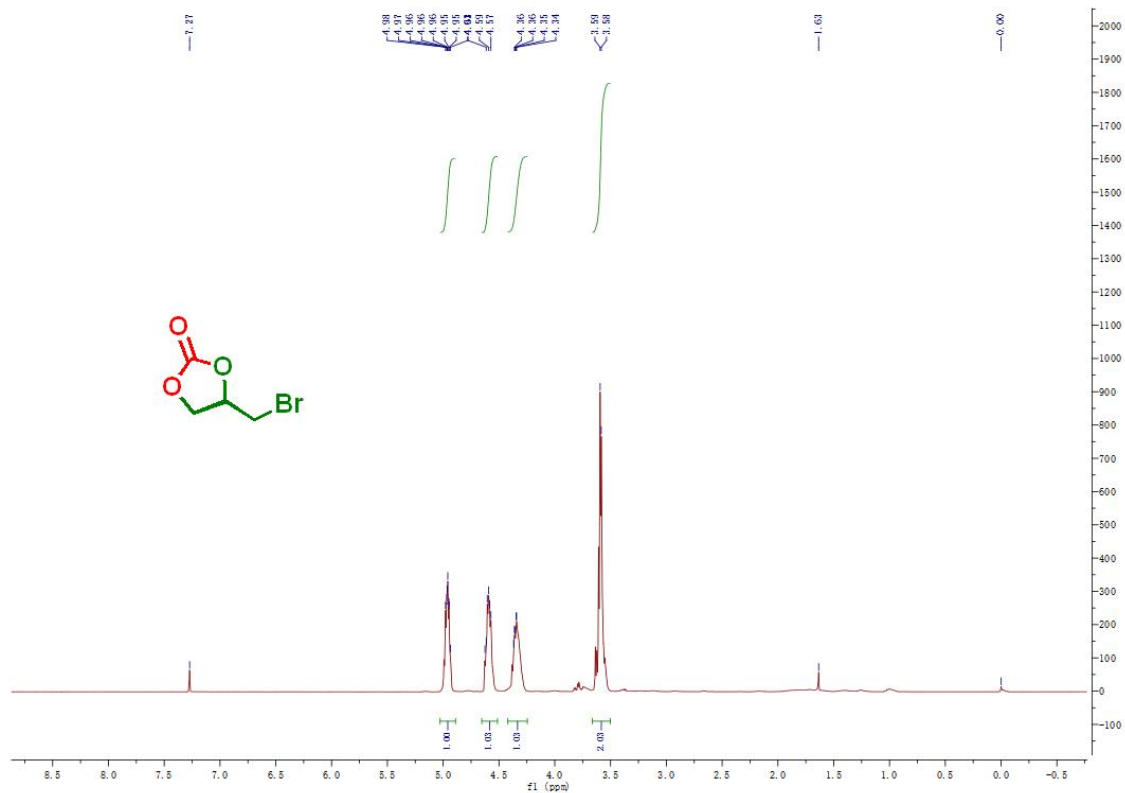
Sample	C (%)	H (%)	N (%)	Cl (%)
HCPs-HQ-Fe	76.58	6.32	1.11	3.16
Recycled	76.25	6.19	1.08	3.04
HCPs-HQ-Fe				

7. Copies of ^1H NMR spectra for compounds 2

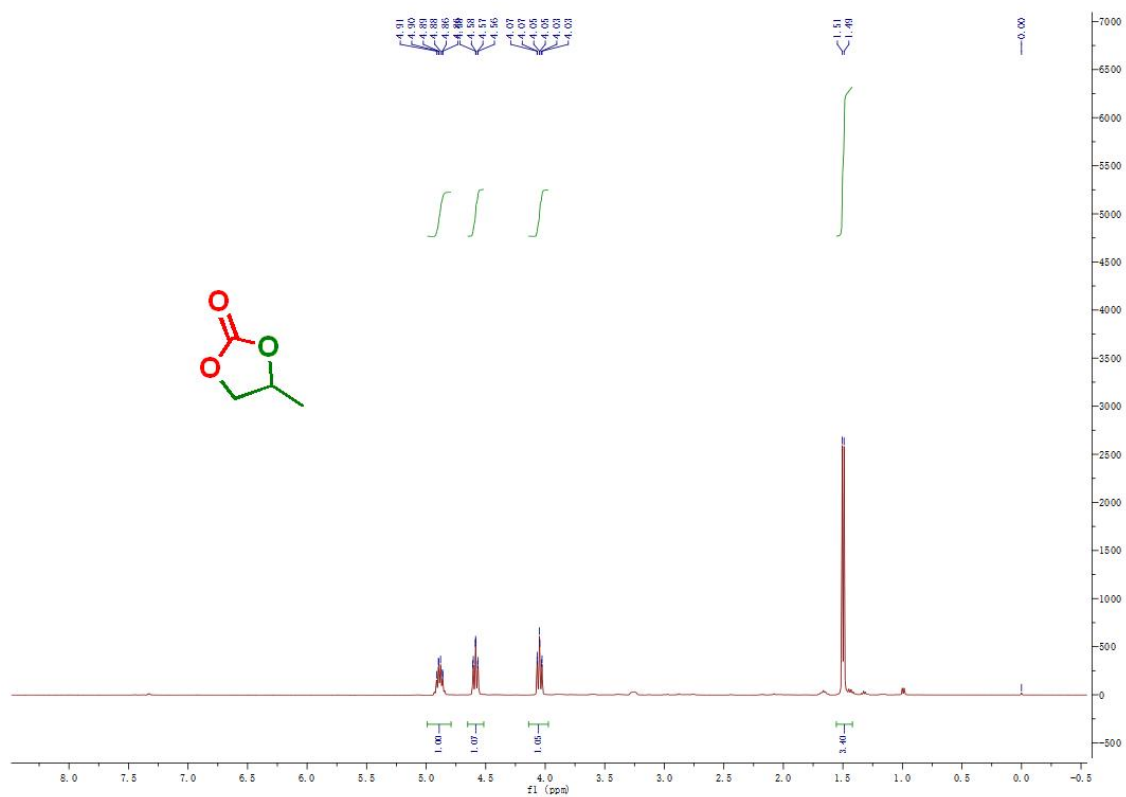
Compound 2a: 4-(chloromethyl)-1,3-dioxolan-2-one.



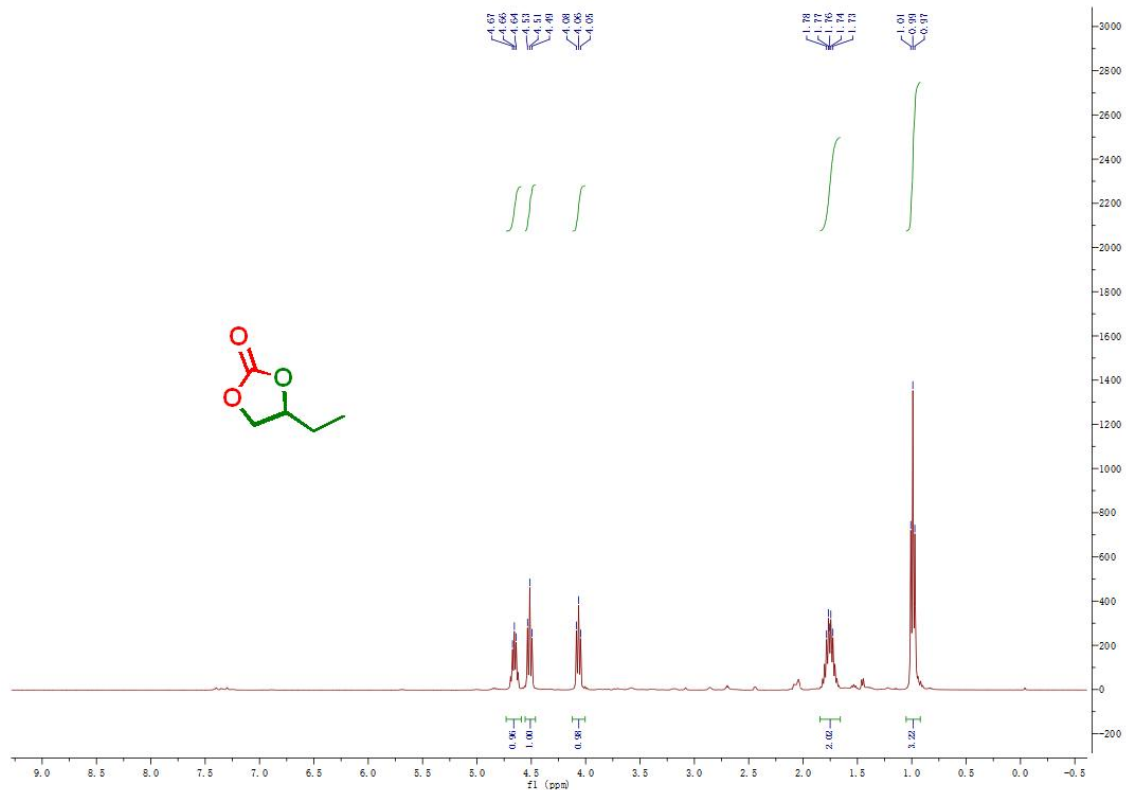
Compound 2b: 4-(bromomethyl)-1,3-dioxolan-2-one



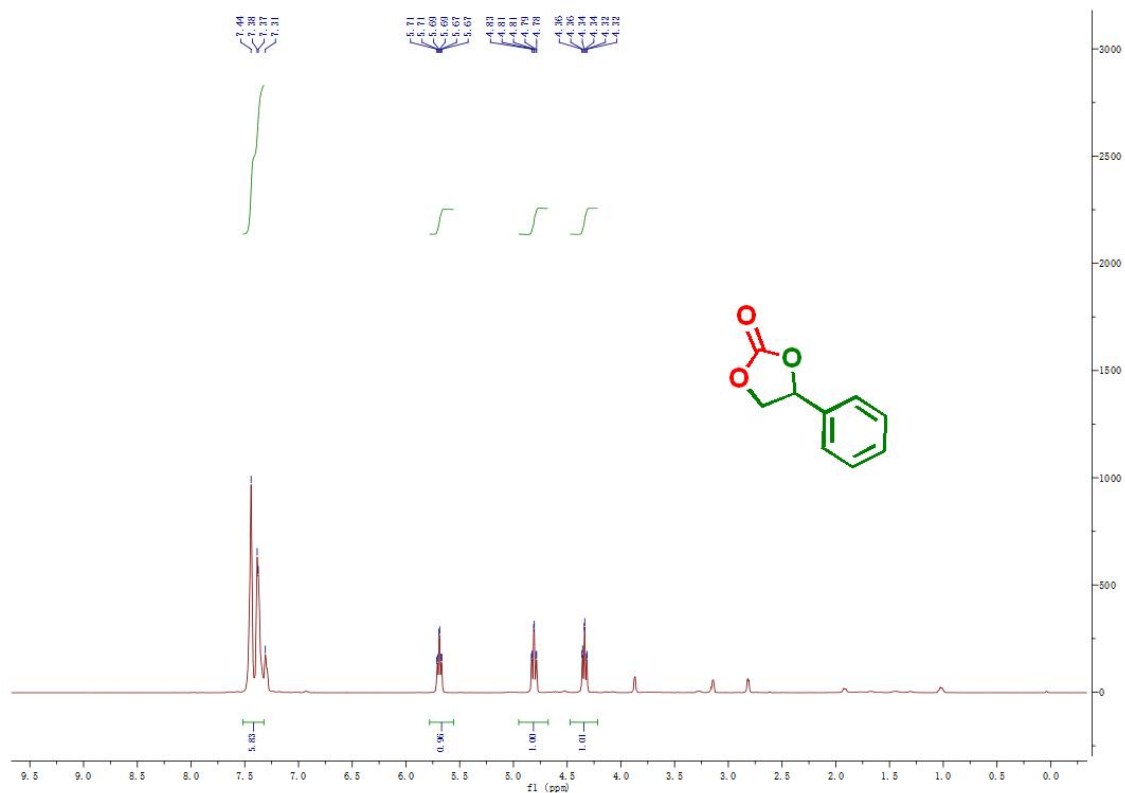
Compound 2c: 4-methyl-1,3-dioxolan-2-one



Compound 2d: 4-ethyl-1,3-dioxolan-2-one



Compound 2e: 4-phenyl-1,3-dioxolan-2-one



Compound 2f: 4-(phenoxy)methyl-1,3-dioxolan-2-one

